Treasures at UT Dallas

UT DALLAS | Eugene McDermott Library

School of Natural Sciences and Mathematics

2011-12-16

Preparation and Characterization of Hybrid Conducting Polymer-Carbon Nanotube Yarn

Javad Foroughi, *et al.*

© 2012 The Royal Society of Chemistry. This paper may not be made further available or distributed without the permission of the copyright owner,

Further information may be found at: http:// http://libtreasures.utdallas.edu/xmlui/handle/10735.1/2500

This document has been made available through Treasures at UT Dallas, a service of the Eugene McDermott Library. Please contact libwebhelp@utdallas.edu for additional information.

Nanoscale

Cite this: *Nanoscale*, 2012, **4**, 940

www.rsc.org/nanoscale

PAPER

Preparation and characterization of hybrid conducting polymer–carbon nanotube yarn†

Javad Foroughi,[a] Geoffrey M. Spinks,*[a] Shaban R. Ghorbani,[b] Mikhail E. Kozlov,[c] Farzad Safaei,[d] Germanas Peleckis,[e] Gordon G. Wallace[a] and Ray H. Baughman[c]

Received 25th October 2011, Accepted 25th November 2011
DOI: 10.1039/c2nr11580h

Hybrid polypyrrole (PPy)–multi walled carbon nanotube (MWNT) yarns were obtained by chemical and electrochemical polymerization of pyrrole on the surface and within the porous interior of twisted MWNT yarns. The material was characterized by scanning electron microscopy, electrochemical, mechanical and electrical measurements. It was found that the hybrid PPy-MWNT yarns possessed significantly higher mechanical strength (over 740 MPa) and Young's modulus (over 54 GPa) than the pristine MWNT yarn. The hybrid yarns also exhibited substantially higher electrical conductivity (over 235 S cm^{-1}) and their specific capacitance was found to be in excess of 60 F g^{-1}. Measurements of temperature dependence of electrical conductivity revealed semiconducting behaviour, with a large increase of band gap near 100 K. The collected low temperature data are in good agreement with a three-dimensional variable range hopping model (3D-VRH). The improved durability of the yarns is important for electrical applications. The composite yarns can be produced in commercial quantities and used for applications where the electrical conductivity and good mechanical properties are of primary importance.

1. Introduction

Electronic textiles that incorporate functional elements such as energy storage and harvesting, sensors and actuators are limited by the difficulty in preparing textile fibres that combine excellent mechanical properties with needed multi-functionality. Recently developed multi-walled carbon nanotube (MWNT) yarns[1] illustrate how a small fraction of MWNTs can be combined with up to 95 weight percent of nano-powders to give continuous lengths of strong yarn fibers suitable for textile processing. The added nano-powders facilitates applications of the textiles for catalysis, battery electrodes, solar cells, photovoltaics and other areas. Separately, the twisted topography of CNT yarns can produce a large and fast rotating type of torsional carbon nantube artificial muscle[2] as a result of volume dilation during electrochemical charge injection. The unique features of these twisted yarns combined with their inherently high electronic conductivity and excellent mechanical properties offers great potential for the further development of electronic textiles.

In this paper we explore a new type of conductive composite prepared by the polymerization of a conductive polymer within and on the surface of MWNT yarns. The developed preparation procedure is substantially different from conventional composite fabrication processes in which polymer and carbon nanotube fillers are mixed and then shaped to form a fiber or film. In our case, the PPy binder was incorporated into the pre-formed MWNT yarn from solution using either electrochemical or chemical polymerization of pyrrole monomer. The composite yarn exhibited improved mechanical, electrical and electrochemical properties as compared with the pristine MWNT material. The composite yarns also exceed the performance of polypyrrole (PPy) and polyaniline fibers.[3–10] The hybrid PPy-MWNT yarns prepared by our method have much higher CNT loading (over 50 wt %) than previously reported polypyrrole and polyaniline and CNT composite fibers[8,11] and possess much higher Young's modulus and electrical conductivity as a result. The composite yarns can be produced in commercial quantities and used for applications where the electrical conductivity along with excellent mechanical properties are of primary importance.

2. Results and discussion

2.1. Morphology of PPy-CNT yarn

SEM micrographs of the pristine CNT yarns are shown in Fig. 1 (a–b). As can be seen from the surface morphology, the

[a]*ARC Centre of Excellence for Electromaterials Science, Intelligent Polymer Research Institute, University of Wollongong, Wollongong, NSW, 2519, Australia. E-mail: gspinks@uow.edu.au*
[b]*Department of Physics, Sabzevar Tarbiat Moallem University, P.O. Box 397 Sabzevar, Iran*
[c]*Alan G MacDiarmid NanoTech Institute, University of Texas at Dallas, Richardson, TX, 75083, USA*
[d]*ICT Research Institute, University of Wollongong, Australia*
[e]*Institute for Superconducting and Electronic Materials, University of Wollongong, Wollongong, New South Wales, 2522, Australia*
† Electronic supplementary information (ESI) available. See DOI: 10.1039/c2nr11580h

This journal is © The Royal Society of Chemistry 2012

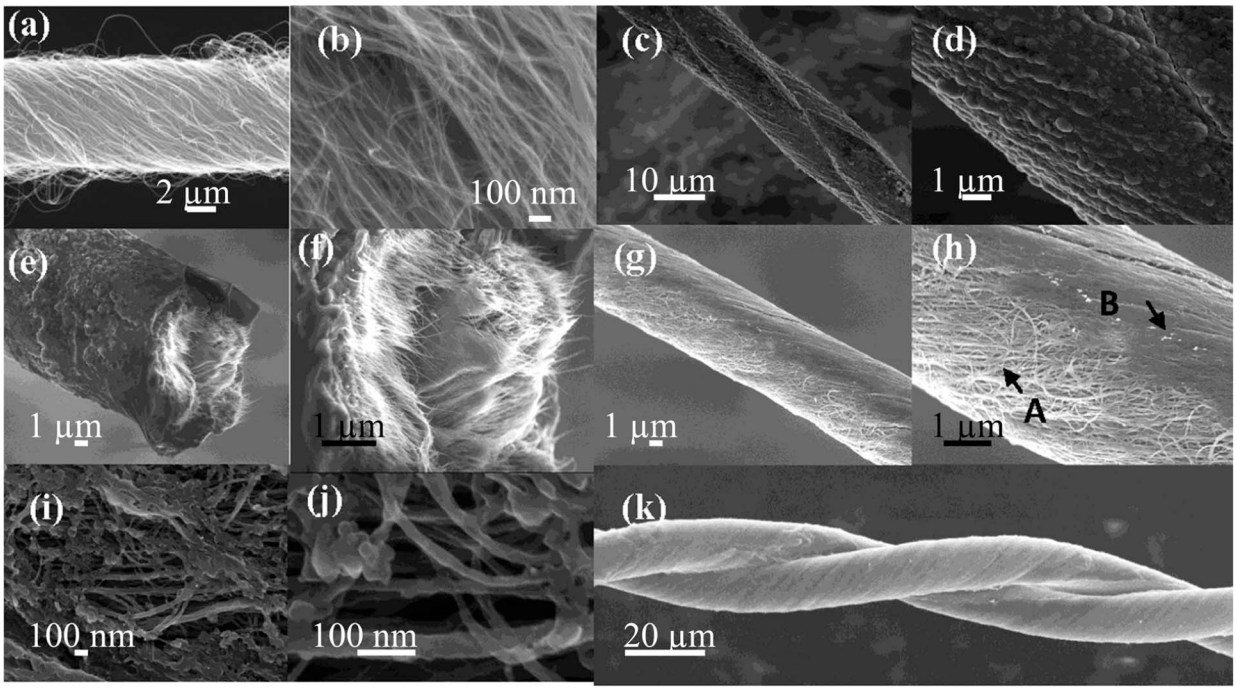

Fig. 1 SEM micrographs of pristine CNT yarn at (a) low and (b) higher magnification; SEM micrographs of electrochemically prepared PPy-CNT yarn showing the surface morphology of a two-ply PPy-CNT at (c) low and (d) higher magnification and (e–f) single yarn in cross-section; SEM micrographs of chemically prepared PPy-CNT yarn showing the surface morphology at (g) low and (h) higher magnification. The higher magnification micrographs in (i) and (j) were taken from region B and A from part (h), respectively. Image (k) shows a longer sequence of the two-ply electrochemically prepared PPy-CNT yarn.

nanotubes were uniform, and predominantly oriented with a helix angle (α) of ~25° to the yarn axis. The electrochemically prepared PPy-CNT yarn showed a core-sheath structure with a CNT inner core and a PPy sheath. The sheath thickness was 25–30 μm (Fig. 1(c–f)) and little PPy deposition occurred inside the MWNT yarn. The surface morphology of electrochemically polymerized PPy-CNT yarns was slightly rough and typical of PPy prepared in this way.[4] SEM micrographs of the chemically prepared PPy-CNT yarn show a non-uniform coating of PPy (Fig. 1(g–h)). Some areas of the yarns displayed a surface morphology similar to that of the pristine CNT yarn, suggesting little incorporation of PPy. These areas are labelled A in Fig. 1(h). In other parts of the yarn, the surface was less porous and CNTs were only visible at higher magnifications. In these regions (region B in Fig. 1(h)) it is apparent that the PPy had penetrated the surface pores and coated the CNTs. This non-uniform coverage of PPy may be due to drying of the oxidant solution giving a thicker oxidant coating on the underside of the yarn that was held horizontally during drying. Further optimization of the drying process could produce a more even coating.

2.2. Mechanical and electrical properties of PPy-CNT yarn

The mechanical properties of CNT and PPy-CNT yarns are shown in Fig. 2. Stress-strain curves obtained from three separate samples from each of the single CNT yarn (1-ply) and chemically prepared PPy-CNT (1-ply) yarn showed a significant difference in mechanical properties. Analysis of these curves indicates a stress at break of 460 ± 20 MPa with 5 ± 2% strain for the single CNT yarn, compared with 510 ± 7 MPa stress with 2.5 ± 0.4% strain for the chemically prepared single PPy-CNT yarn. Young's modulus of these yarns was 12 ± 2 GPa and 35 ± 3 GPa for the CNT yarn and chemically prepared PPy-CNT yarn, respectively. It is expected that PPy in the PPy-CNT yarn reduces the slippage between CNT bundles, thereby increasing the shear resistance and elastic modulus. The effect of the preparation method on mechanical properties of PPy-CNT yarn was investigated using the two-ply twisted yarns. The chemically prepared two-ply PPy-CNT yarn showed significantly higher mechanical properties than the electrochemically prepared composite, with a stress at break of 740 ± 18 MPa at 1.5 ± 0.6% strain compared with 273 ± 9 MPa stress at 4.5 ± 1% strain for the electrochemically prepared two-ply PPy-CNT yarn. The Young's modulus of these yarns was 57 ± 6 GPa and 7.6 ± 0.4 GPa for the chemically and electrochemically prepared PPy-CNT yarns,

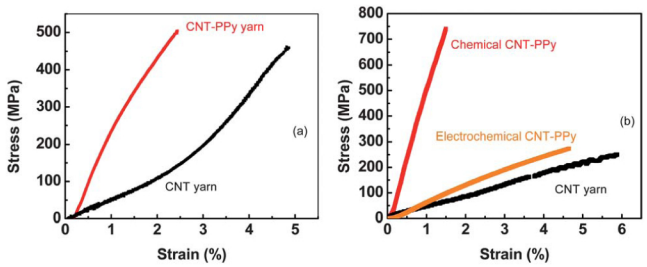

Fig. 2 (a) Stress *vs.* strain curves for (a) single-ply MWNT yarn and chemically prepared single-ply PPy-MWNT yarn; and (b) chemically and electrochemically prepared two-ply PPy-CNT and pristine two-ply CNT yarns.

respectively. The significant increase in modulus over the pristine CNT yarn is consistent with the PPy forming inside the yarn and acting to bind the MWNT bundles together in the case of the chemically prepared PPy-CNT yarn. In contrast, the electrochemically developed PPy-CNT yarn exhibited a significantly lower modulus than the chemically developed PPy-CNT yarn but similar to the 2-ply pristine CNT yarn. Since the electrochemically prepared PPy has little effect on the CNT yarn modulus, it is likely that little PPy forms within the CNT yarn pores. Electrochemical polymerization appears to occur preferentially on the surface of the yarn. As such, the PPy deposited electrochemically does not alter the internal yarn structure and the mechanical properties are not significantly affected.

Fig. 3(a) compares the temperature dependence of the conductivity, σ(T), for the CNT yarn and the electrochemically and chemically prepared PPy-CNT yarns. The room temperature conductivity of the three samples studied here are 176 ± 10, 220 ± 9, and 235 ± 15 S cm^{-1}, respectively. The conductivity of all samples decreased linearly with decreasing temperature down to T ≈ 100 K and then decreased more sharply as the temperature decreased further. The transport properties of the conducting polymer can be characterized by slope of the temperature dependence of the reduced activation energy defined as[12]

$$W(T) = -d\ln(\rho(T))/d\ln(T) = d\ln(\sigma(T))/d\ln(T) \quad (1)$$

The W(T) of the CNT yarn and the electrochemically and chemically prepared PPy-CNT yarns are compared in Fig. 3(b). As can be seen there is a shape change in activation energy at T ≈ 100 K. The conductivity shows a power-law dependence on temperature, *i.e.*[13]

$$\sigma(T) \sim T^{\beta} \quad (2)$$

where β varies from 0.3 in the low temperature regime to 1 in the high temperature regime. At temperatures higher than 100 K, $\beta = 1$, which implies that these materials are in the low band gap state. For insulating samples, the temperature dependence of the conductivity of conducting polymers is commonly explained by an exponential temperature dependence characteristic of a variable range hopping (VRH) model[14]

$$\sigma(T) = \sigma_0 \exp[(-T_0/T)^{1/(1+d)}] \quad (3)$$

where σ_0 is the high temperature limit of dc conductivity and T_0 is related to thermally activated hopping among localized states and d is the dimensionality of the conduction process of the system. Fig. 3(c) shows $\ln\sigma(T)$ *vs.* $T^{-1/(1+d)}$ with $d = 3$ at low temperature, *i.e.* T < 100 K, for the CNT yarn and the electrochemically and chemically prepared PPy-CNT yarns. The conductivity is evaluated from the best-fitted straight lines as presented in Fig. 3(c). the $\ln\sigma(T)$ as a function of $T^{-1/(1+d)}$ with $d = 1$ and 2 does not exhibit a good linear fit (see supporting information†). Therefore, the conductivity does not correspond to a one or two dimensional variable range hopping (VRH) model. Fig. 3(c) shows that $\ln\sigma(T)$ *versus* $T^{-1/(1+d)}$ with $d = 3$ gives a straight line. These results indicate that the transport mechanisms correspond to a 3D-VRH model in all three samples. The best-fitted values of T_0, which can be interpreted as the effective energy separation between localized states, and σ_0 for 3D-VRH model are shown in Table 1 for the three samples. The results show that T_0 for the CNT yarn (2.14 K) is larger than those for both the electrochemically and chemically prepared PPy-CNT yarns (≈1.1 K) by a factor 2. Therefore, the effective energy separations between localized states of the electrochemically and chemically prepared PPy-CNT yarn samples are smaller than those for pristine CNT yarn. This conclusion is supported by increasing σ_0. The T_0 for three-dimensional hopping transport is given by

$$T_0 = \frac{16}{k_B L^3 N(E_F)} \quad (4)$$

where L is the localization length and $N(E_F)$ is the density of states at the Fermi level. The disorder degree of the systems reduces with lowering of T_0 because T_0 is inversely proportional to L. The values of L are calculated by considering the charge transport primarily arising from the conducting polypyrrole phase and assuming $N(E_F)$ of about 7.5×10^{19} $eV^{-1}.cm^{-3}$.[15] The localization length L values are shown in Table 1 for the three samples. The localization length for the CNT yarn is about 105 nm while for the both PPy-CNT yarns it increases to about 130 ± 2 nm. The average hopping distance (R_{hop}) between two sites and the activation energy (W_{hop}) are given by

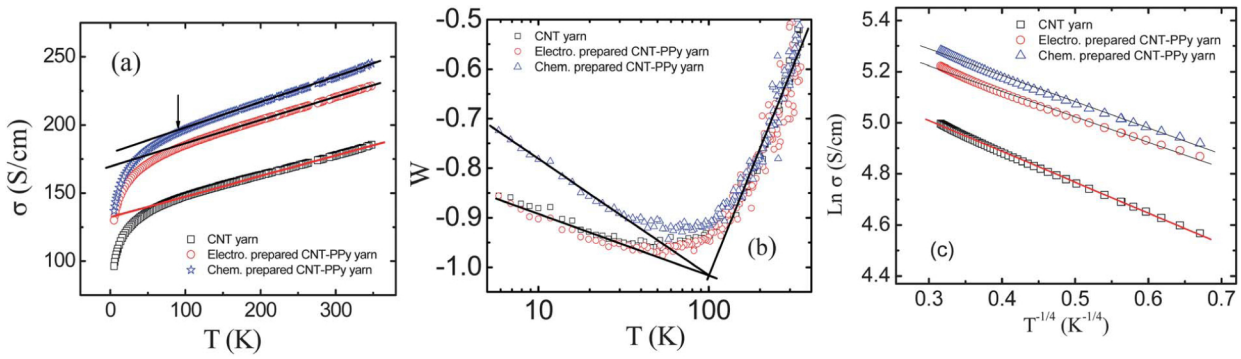

Fig. 3 (a) The temperature dependence of σ (T) of the 3 CNT yarn test samples. (b) The temperature dependence of reduced activation energy W(T) of the 3 CNT yarn test samples and (c) Ln σ *vs.* T − 1/(1 + d) (d = 3, 3D-VRH) of the CNT yarn and the electrochemically and chemically prepared PPy-CNT yarns.

This journal is © The Royal Society of Chemistry 2012

Table 1 Conductivity analysis for the 3 CNT yarn test samples

Sample	T_0 (K)	σ_0 (S cm^{-1})	L (nm)	R_{hop} (nm)	W_{hop} (meV)
CNT yarn	2.14	215.1	105	11.5	1.88
Electrochem. PPy-CNT yarn	1.05	252.0	133	12.2	1.57
Chemical PPy-CNT yarn	1.18	270.8	128	12.0	1.62

$$R_{hop} = (3/8)(T_0/T)^{1/4}\, L \quad (5)$$

$$W_{hop} = (1/4)k_B T(T_0/T)^{1/4} \quad (6)$$

At room temperature, the average hopping distance for the CNT yarn is about 11.5 nm while for the both PPy-CNT yarns it increases to about 12 nm. These distances corresponds to about 35–40 monomer units in length. The estimated activation energies for hopping are 1.88 meV and ≈1.60 meV for the CNT yarn and PPy-CNT yarn, respectively (as shown in Table 1). This is in good agreement with the average hopping distance changes.

2.3. Magnetoresistance

Fig. 4(a) shows the magnetoresistance, MR = (ρ(H) − ρ(0))/ρ(0) *100%, as a function of magnetic field at different temperatures for pristine CNT yarn sample (see supporting information for other samples†). The MR was negative and large at low temperatures for all samples. The MR was weakly field dependent at magnetic fields (B) lower than 1.1 T and then decreased with increasing field strength. At $T = 5$ K and B = 10 T, MR was −16.6, −15.3, and −15.4 for CNT yarn and electrochemically and chemically prepared PPy-CNT yarns, respectively. In the three samples, the MR increased strongly with increasing temperature at B = 5 and 10 T (Fig. 4(b)); however, the initial increase was followed by saturation at high temperatures. As can be seen in Fig. 4(b), the MR does not vary between samples at temperature lower than 250 K and B = 5 T while at B = 10 T the MR was found to be both field and sample dependent. The MR data are replotted *vs.* $B^{1/2}$ in Fig. 4(c). There are two different regions in the magnetic dependence of magnetoresistance. At fields smaller than the crossover field, $B^* = 1.1$ T, which is temperature and sample independent, the MR was constant at temperatures used in this work for all samples. The MR decreased linearly when the magnetic field was larger than B^*. However, the slope of MR *vs.* $B^{1/2}$ strongly deceases with increasing temperature (see supporting information for other samples†). It was found that external magnetic fields affect localization and electron correlation in disordered materials.[16] The contribution to the magnetoresistance due to electron-electron interaction is positive while the sign of the magnetoresistance associated with localization can be negative or positive depending on spin–orbit effects.[17] A magnetic field gives a negative MR[18] when spin–orbit effect is weak and a positive MR[19] when spin–orbit scattering is strong. Our results show that the electron correlation is not important in these materials due to a negative MR and that localization is due to weak spin–orbit scattering.

2.4. Electrochemical properties of PPy-CNT yarn

The electroactivity of the three yarn samples was also determinedwith cyclic voltammograms (CVs) shown in Fig. 5. Reasonable electroactivity was observed for the PPy-CNT yarns in 0.10M Li.TFSI in propylene carbonate, as evidenced by oxidation and reduction peaks at ~0.3 and −0.4 V (Ag/Ag$^+$ reference), respectively. Furthermore, the electrochemically developed PPy-CNT yarn exhibited more electroactive behaviour and clearly exhibited oxidation and reduction peaks, possibly due to having more PPy incorporated onto the CNT yarn compared to the chemically prepared CNT yarn. The gravimetric capacitance of the pristine CNT and chemically and electrochemically prepared PPy-CNT yarns was estimated from the CVs obtained from 3 samples to be 40 ± 2, 59 ± 4 and 53 ± 5 F g^{-1}, respectively, over a potential range of −0.9 to +0.7 V. These results are higher than the capacitance observed for pristine MWNT yarn (26 F g^{-1}) and for single-wall carbon nanotubes.[20,21]

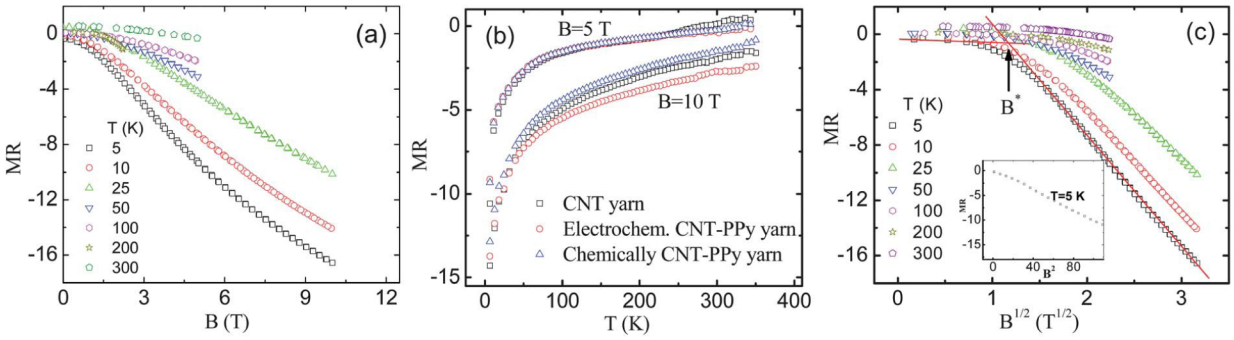

Fig. 4 (a)The magnetoresistance as a function of B at different temperatures for pristine CNT yarn, (b) The magnetoresistance as a function of temperature at B = 10 T for the three CNT yarn test samples and (c) magnetoresistance *vs.* $B^{1/2}$ for pristine CNT yarn. Lines shown to act as a guide. The arrow shows the crossover field B^*.

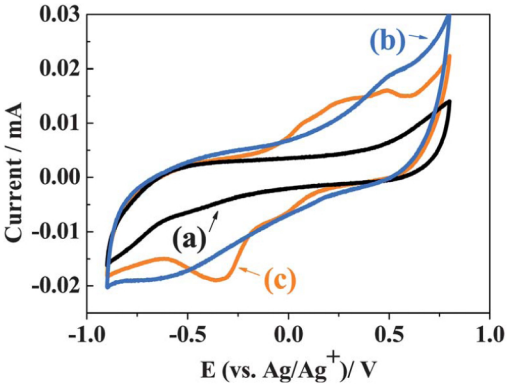

Fig. 5 Cyclic voltammograms of (a) pristine CNT, (b) chemically prepared PPy-CNT, (c) electrochemically prepared PPy-CNT yarns. Potential was scanned between −0.9 and +0.7 V (*vs.* Ag/Ag^+) in 0.10 M Li.TFSI in PC at 100 mVs^{-1}.

3. Conclusions

The preparation and characterization of hybrid PPy-CNT yarns has been successfully achieved using chemical and electrochemical polymerization of pyrrole. Single and two-ply multi-walled carbon nanotube yarns were used to develop the PPy-CNT yarn. SEM micrographs of the pristine CNT and PPy-CNT yarns were carried out to reveal a core-sheath structure for the electrochemically prepared PPy-CNT yarn. However, chemically developed PPy-CNT yarn had a heterogeneous morphology consisting of dense regions of PPy-infiltrated CNT and more porous areas having less PPy. The chemically prepared PPy-CNT yarn exhibited a much higher stress at break (740 MPa) and Young's modulus (54 GPa) compared with the pristine MWNT yarn. Electrical properties of pristine CNT yarn and PPy-CNT yarns were characterised. The effective energy separation between localized states of the pristine CNT yarn (2.14 K) is larger than that for both the electrochemically and chemically prepared PPy-CNT yarn (1.1 K) indicating different electrical properties. All three yarns show variation of activation energy with temperature with drastic increase of band gap below $T \approx 100$ K. The conductivity results are in good agreement with the conductivity analyses in the frame of a 3D-VRH model at low temperatures. The magnetoresistance is negative and large at low temperatures and it is weakly field dependent at fields lower than 1.1 T and then decreases with field strength. The MR increases strongly with increasing temperature; however, the initial increase is followed by saturation at high temperatures. These results suggest that the newly developed PPy-CNT yarns may be useful for some applications such as actuators, sensors and batteries.

4. Experimental

The MWNT forest was synthesized by catalytic CVD (chemical vapour deposition) using acetylene gas as the carbon source.[22] Carbon nanotubes in the forest typically had a diameter of about 10 nm. The yarn was drawn from the forest by pulling and twisting as described previously.[23] The two-ply yarns were obtained by over twisting the single-ply yarn and then allowing it to relax until it reached a torque-balanced state. The samples used in this work are single-ply MWNT yarn with 6–10 μm diameter and 20000 turns per meter (TPM) inserted twist and two-ply MWNT yarns with 15–20 μm diameter and 16000 TPM inserted twist. The hybrid PPy-MWNT yarn was prepared by electrochemical and chemical polymerization of pyrrole onto the surface of the MWNT yarn. *p*-toluenesulfonate was supplied by Sigma Aldrich and ferric toluenesulfonate (Fe.*p*TS) in n-butanol (40% v/v) (Clevios C-B40) was supplied by H.C. Starck and were used as received. Pyrrole monomer (95%, Aldrich) was used after distillation.

PPy-CNT yarns were produced by chemical polymerization of pyrrole through vapour phase polymerization, as described in detail in the Supporting Information.† A comparison of the weight of sample before and after polymerization indicated that the weight fraction of the PPy in the PPy-CNT yarn was ~8 wt%. In addition, polypyrrole was incorporated into the CNT yarn successfully by anodic oxidation of pyrrole monomer. A comparison of the weight of sample before and after polymerization indicated that the weight fraction of PPy in PPy-CNT yarn was ~74 wt%. Two ply PPy-CNT also prepared to investigate effect of fabrication on mechanical properties. Raman spectra of the MWNT yarn and PPy-CNT yarn showed that pyrrole was successfully polymerized on to the CNTs. Tensile testing was carried out using a TA instrument Dynamic Mechanical Analyser. A 10 mm gauge length of yarn was stretched at a strain rate of 500 μm min^{-1} until the sample broke at 25 °C. To obtain accurate result for mechanical properties 3 samples were tested. Cyclic voltammetry studies were carried out using a three electrode electrochemical cylindrical cell (15 mm × 50 mm) coupled to a Bioanalytical Systems (Model CV27) potentiostat. A 10 mm yarn was used as the working electrode with an Ag/Ag^+ reference electrode and a Pt mesh counter electrode. A Leica Stereoscan 440 Scanning Electron Microscope (SEM) was employed for morphological studies. Fibre samples were fractured after cooling in liquid N_2 to obtain circular undamaged cross-sections. Electrical transport of the carbon nanotubes and PPy-CNT yarns was characterized by standard four probe technique (Quantum Design PPMS). All measured yarns were placed onto MgO substrate and four Au wires were attached to every sample using silver paste. The dependence of resistivity (ρ) on temperature (T) was measured under 0, 5, and 10 Tesla (T) applied magnetic field while sweeping the temperature from 350 K to 5 K with a sweep rate of 3 K min^{-1}. Magnetoresistance (MR), defined as $MR = (\rho(H) - \rho(0))/\rho(0) *100\%$, was obtained by sweeping the magnetic field (H) at set temperatures with a sweep rate of 80 Oe/s.

Acknowledgements

Authors would like to thank The Australia Research Network for Advanced Material (ARNAM), the Australian National Fabrication Facility and the Australian Research Council through the Centres of Excellence scheme for financial support. The authors also thank Anthony Charles Romeo for his assistance with electron microscopy.

References

1 M. D. Lima, S. Fang, X. Lepro, C. Lewis, R. Ovalle-Robles, J. Carretero-González, E. Castillo-Martínez, M. E. Kozlov, J. Oh,

 This journal is © The Royal Society of Chemistry 2012

N. Rawat, C. S. Haines, M. H. Haque, V. Aare, S. Stoughton, A. A. Zakhidov and R. H. Baughman, *Science*, 2011, **331**, 51–55.
2 J. Foroughi, G. M. Spinks, G. G. Wallace, J. Oh, M. E. Kozlov, S. Fang, T. Mirfakhrai, J. D. W. Madden, M. K. Shin, S. J. Kim and R. H. Baughman, *Science*, 2011, **334**, 494–497.
3 J. Foroughi, G. M. Spinks, G. G. Wallace and P. G. Whitten, *Synth. Met.*, 2008, **158**, 104–107.
4 J. Foroughi, S. R. Ghorbani, G. Peleckis, G. M. Spinks, G. G. Wallace, X. L. Wang and S. X. Dou, *J. Appl. Phys.*, 2010, **107**, 103712–103714.
5 J. Foroughi, G. M. Spinks and G. G. Wallace, *Synth. Met.*, 2009, **159**, 1837–1843.
6 J. Foroughi, G. M. Spinks and G. G. Wallace, *J. Mater. Chem.*, 2011, **21**, 6421–6426.
7 J. Foroughi, G. M. Spinks and G. G. Wallace, *Sens. Actuators, B*, 2011, **155**, 278–284.
8 V. Mottaghitalab, G. M. Spinks and G. G. Wallace, *Polymer*, 2006, **47**, 4996–5002.
9 N. G. Sahoo, Y. C. Jung, H. H. So and J. W. Cho, *Synth. Met.*, 2007, **157**, 374.
10 N. G. Sahoo, Y. C. Jung, H. J. Yoo and J. W. Cho, *Compos. Sci. Technol.*, 2007, **67**, 1920.
11 J. Foroughi, PhD, University of Wollongong, 2009.
12 R. Menon, C. O. Yoon, D. Moses, A. J. Heeger and Y. Cao, *Phys. Rev. B: Condens. Matter*, 1993, **48**, 17685.
13 C. O. Yoon, R. M. D. Moses and A. J. Heeger, *Phys. Rev. B: Condens. Matter*, 1994, **49**, 10851.
14 N. F. Mott and E. A. Davis, *Electronic Processes in Non-Crystalline Materials*, Oxford, Clarendon, 1979.
15 B. R. Saunders, K. S. Murray and R. J. Fleming, *Synth. Met.*, 1992, **47**, 167–178.
16 P. A. Lee and T. V. Ramakrishnan, *Rev. Mod. Phys.*, 1985, **57**, 287.
17 P. Dai, Y. Zhang and M. P. Sarachik, *Phys. Rev. B: Condens. Matter*, 1992, **46**, 6724.
18 A. Kawabata, *J. Phys. Soc. Jpn.*, 1980, **49**, 628–637.
19 S. Hikami, A. I. Larkin and Y. Nagaoka, *Prog. Theor. Phys.*, 1980, **63**, 707–710.
20 M. Hughes and G. M. Spinks, *Adv. Mater.*, 2005, **17**, 443–446.
21 M. Tissaphern, *et al.*, *Smart Mater. Struct.*, 2007, **16**, S243.
22 K. R. Atkinson, S. C. Hawkins, C. Huynh, C. Skourtis, J. Dai, M. Zhang, S. Fang, A. A. Zakhidov, S. B. Lee, A. E. Aliev, C. D. Williams and R. H. Baughman, *Phys. B*, 2007, **394**, 339–343.
23 M. Zhang, K. R. Atkinson and R. H. Baughman, *Science*, 2004, **306**, 1358–1361.